J Biosci (2019) 44:145
DOI: 10.1007/s12038-019-9950-y

Investigation of axonal regeneration of *Triturus ivanbureschi* by using physiological and proteomic strategies

Seçil Karahisar Turan[1], Mehmet Ali Onur[1] and Fatma Duygu Özel Demiralp[2]*

[1]*Department of Biology, Faculty of Science, Hacettepe University, 06800 Ankara, Turkey*

[2]*Department of Biomedical Engineering, Faculty of Engineering, Ankara University, 06830 Ankara, Turkey*

**Corresponding author (Email, ozeldemiralp@gmail.com)*

MS received 12 February 2019; accepted 16 July 2019; published online 31 October 2019

Peripheral nerve injuries are frequently observed and successful treatment depends mainly on the injury type, location of the damage, and the elapsed time prior to treatment. The regenerative capacity is limited only to the embryonic period in many mammalian tissues, but urodele amphibians do not lose this feature during adulthood. The main purpose of this study is to define the recovery period after serious sciatic nerve damage of a urodele amphibian, *Triturus ivanbureschi*. Experimental transection damage was performed on the sciatic nerves of *T. ivanbureschi* specimens. The recovery period of sciatic nerves were investigated by walking track analysis, electrophysiological recordings, and bottom-up proteomic strategies at different time points during a 35-day period. A total of 34 proteins were identified related to the nerve regeneration process. This study showed that the expression levels of certain proteins differ between distal and proximal nerve endings during the regeneration period. In distal nerve stumps, transport proteins, growth factors, signal, and regulatory molecules are highly expressed, whereas in proximal nerve stumps, neurite elongation proteins, and cytoskeletal proteins are highly expressed.

Keywords. Axonal regeneration; electrophysiology; proteomics; urodele; walking track analysis

1. Introduction

The potential to regenerate lost or damaged tissues and organs differ between animal phyla. Primary examples are seen in most animals including cnidarians, annelids, mollusks, planarians, and even chordates. Urodeles are known for their high regenerative capacity among chordates (Tsonis 2002).

Neural regeneration and reinnervation of target tissues are affected by numerous factors such as the neuronal type, growth environment, and target. Axon regeneration is a process where a cell projection should grow through a long substrate (Carlson 2007). After peripheral nerve damage, neurotrophic factors are expressed and released from several areas including target tissues, neural somas, glial cells, fibroblasts, macrophages, and Schwann cells. Surviving neurons switch from a growth mode to transmitting mode and conduct morphological, physiological and molecular changes (Fu and Gordon 1997; Zochodne 2008).

Distal and proximal nerve stumps react differently after peripheral nerve axotomy. The growth environment in the nerve stump distal to the damaged area should provide adequate support, and the regenerating axon should reinnervate the proper target organ, which maintains the capacity of reinnervation and releasing from denervation atrophy (Fu and Gordon 1997).

Axotomy causes many modifications both in distal and proximal nerve stumps. In a surviving nerve after an injury, the nerve stump proximal to the lesion generally degenerates until the first node of Ranvier with the effect of calcium influx and activation of calcium-associated proteases. Proximal stumps swell by the effect of cytoskeletal proteins and organelles which transport there via slow and fast axoplasmic transport. The damaged axon needs a growth cone which elongates dynamically. Local protein synthesis induces these preliminary modifications without the contribution of transcriptional events. Preexisting cytoskeletal elements in axons are transported to the daughter axons that start to grow from the proximal nerve stump. Microtubules function like bridges, which transport essential materials for axonal elongation between old axons and emerging ones. Regenerating axon stumps begin to elongate from the first node of Ranvier proximal site of the lesion. These fine nerve fibers elongate towards to distal nerve stump through the supportive microenvironment of distal nerve sprouts (Fu and Gordon 1997; Zochodne 2008).

The growth environment of the distal nerve stump is important for successful peripheral nerve regeneration. Regenerating axons grow toward denervated targets in endoneural tubes organized by intact axons and the myelin sheath. The primary changes in the distal nerve stump are degenerative and are

associated with "Wallerian degeneration," which removes axonal fragments and myelin debris. At the end of this process, a distal nerve stump remains that consists of connective tissue scaffolds and supportive Schwann cells (Fu and Gordon 1997; Rodríguez *et al.* 2004; Zochodne 2008).

Molecules with direct or indirect effects on axonal regeneration can be generally classified as neurotrophic factors, cell adhesion molecules and extracellular matrix proteins (Fu and Gordon 1997). Toward understanding regenerative mechanisms, crucial approaches include defining the role of local protein synthesis and post-translational modifications in neural regeneration by obtaining protein profiles and determining altered protein amounts.

Mass spectrometry-based proteomics are generally used in neuroscience to investigate differences in protein expression, protein-protein interactions, and post-translational modifications. Proteomic approaches are needed to understand neural regeneration mechanisms, which are based on axonal transport, cytoskeletal elements, chaperones and altered signaling pathways (Kiffmeyer *et al.* 1991; Michaelevski *et al.* 2010). Because of the complexity of the nervous system, including its heterogeneous cell types, complex morphology and anatomy, the application of proteomic studies is challenging. Thus, proteomics-based studies in neural tissues are relatively few (Goto *et al.* 2009).

To the best of our knowledge, an investigation of the newt neural regeneration process using behavioral, electrophysiological, and two-dimensional gel-based bottom-up proteomics, has not been reported. In this study we investigated the regeneration period of newt sciatic nerve tissue. We utilized the crested newt collected from Kastamonu, Turkey as our model. It was previously named *Triturus karelinii* or *Triturus ivanbureschi* until 2013, but was renamed *Triturus anatolicus* in 2016 following molecular analysis (Wielstra and Arntzen 2016). In this study, as this new name is not yet commonly used, we refer to this species as *T. ivanbureschi*. Along with walking track analysis data and compound muscle action potential (CMAP) recordings, we confirmed and showed the recovery process of newt transected nerves. We compared the distal and proximal nerve ending protein profiles and detected statistically significant differences in protein expression levels between different time points ($p<0.05$). We identified 34 proteins related to axonal elongation, cytoskeletal remodeling, and developmental mechanisms.

2. Materials and methods

2.1 *Ethical approval*

All *Triturus ivanbureschi* specimens were collected from their natural habitats with the permission of the Republic of Turkey, Ministry of Forestry and Water Affairs, General Directorate of Nature Conservation and National Parks (protocol B.23.0.DMP.0.15.01-510.02-9165). All experimental procedures were approved by Hacettepe University Animal Research Ethics Committee (protocol B.30.2.HAC.0.05.06.00/17).

2.2 *Animal collection and care*

Adult *Triturus ivanbureschi* specimens were collected from artificial ponds using fish nets during spring from the town called İnebolu, in the Kastamonu province of Turkey. Living specimens were brought to the laboratory in plastic boxes. Animals were kept at 20°C in vivariums and fed tubifex worms at 2-day intervals. The experimental process began after a 2-week acclimation period.

2.3 *Experimental nerve damage*

The experiments were carried out in 36 *Triturus ivanbureschi* specimens of either sex, 12–16 cm in length. Newts were anaesthetized by immersion in 1 g/L ethyl 3-aminobenzoate methanesulfonate (MS-222, Aldrich). All surgical operations were conducted after no response was elicited by tactile stimuli. Both sciatic nerves were exposed at the mid-femoral region; the right sciatic nerves transected at mid-femoral region and constituted the experiment group whereas the left sciatic nerves constituted the sham control group. After surgical operation, all newts were placed in clean water and monitored until the return of normal activity and motility.

2.4 *Walking track analysis*

The recovery process was followed by walking track analysis 0 (3 h), 1, 7, 14, 21 and 35 days post-surgery. The walking track analysis results were used to determine the Sciatic Function Index (SFI) values, which are commonly used to monitor the recovery process in rats. However, there is no common method for tracking the recovery period from behavioral changes in urodele amphibians.

Newts are aquatic amphibians whose swimming skills are better than their walking skills. At the beginning of this study, both swimming and walking patterns were recorded. Unfortunately, significant differences were not observed during the swimming sessions after sciatic nerve damages, therefore walking patterns were used. In this study, the hind feet of newts were stained with a water-based ink and gait analysis was examined through a plexiglass platform. Gait analysis was also recorded with a digital camera placed under the platform. The video recordings were converted to frames to measure the tracks. From these measurements, the SFI and the Static Sciatic Index (SSI) values were calculated as the distance between the toes of the measuring foot to the opposite foot (the distance to the opposite foot, TOF), the distance from the heel to toe (print length, PL), the distance between first and fifth toes (the toe spread, TS) and the

distance between the second and fourth toes (the intermediary toe spread, IT). Walking tracks were recorded in two day intervals for all time points, except the day 0 and 1, until the experiments were terminated. The measurements were analyzed by Image J (NIH, USA) software.

The SFI was determined using walking track data from all newts using the formulas of de Medinaceli *et al.* (1982), Carlton and Goldberg (1986), and Bain *et al.* (1989) and the Static Sciatic Index (SSI) was determined using the formula of Bervar (2000), all of which are typically described for rats. In these formulas, the SFI has a value between zero and −100, which the score of the transected sciatic nerves corresponds to −100, and healthy sciatic nerves are zero (Bain *et al.* 1989). Averaged values from six newts at each time point are used to draw the SFI and SSI graphs (figure 1).

The time points utilized were determined from preliminary results taken up to 44 days after transection of two newt sciatic nerves. On day 35, we observed the joining of separated proximal and distal sciatic nerve endings. From these optimization studies, we investigated the sciatic nerve regeneration over a period of six time points. The first two time points were taken 0 (3 h) and 1 day after damage to establish the injury-induced acute phase reactants. To reduce the number of animals used without affecting the statistical significance, six time points were established which includes 0, 1, 7, 14, 21, and 35 days after sciatic nerve damage.

2.5 *Electrophysiological recordings*

Electrophysiological recordings were performed at 0 (3 h), 1, 7, 14, 21 and 35 days following surgery from both control and damaged legs with BioPac MP35 Data Acquisition System (BioPac Systems, Inc., USA). Compound Muscle Action Potential (CMAP) recordings were obtained from the gastrocnemius muscle by supramaximal stimulation of sciatic nerve (intensity 2.5 V, duration 1 ms, frequency 0.50 Hz, 5–500 Hz, 100 kHz/s with a sampling rate) using needle electrodes. Group averages were calculated after the mean values were obtained for each specimen from ten action potential waves. IBM SPSS Statistics Version 20 software was used for statistical analysis. Descriptive statistics were performed to check for the normal distribution by the Shapiro-Wilk test. Normally distributed continuous variables were compared with one-way ANOVA and post-hoc tests and $p<0.05$ was considered statistically significant.

2.6 *Protein concentration measurement*

Sciatic nerves at approximately 1.5–2.3 mm length were removed from all newts at each time point for proteomic analysis. Sciatic nerves from six newts were pooled for each time point to obtain adequate protein concentration for

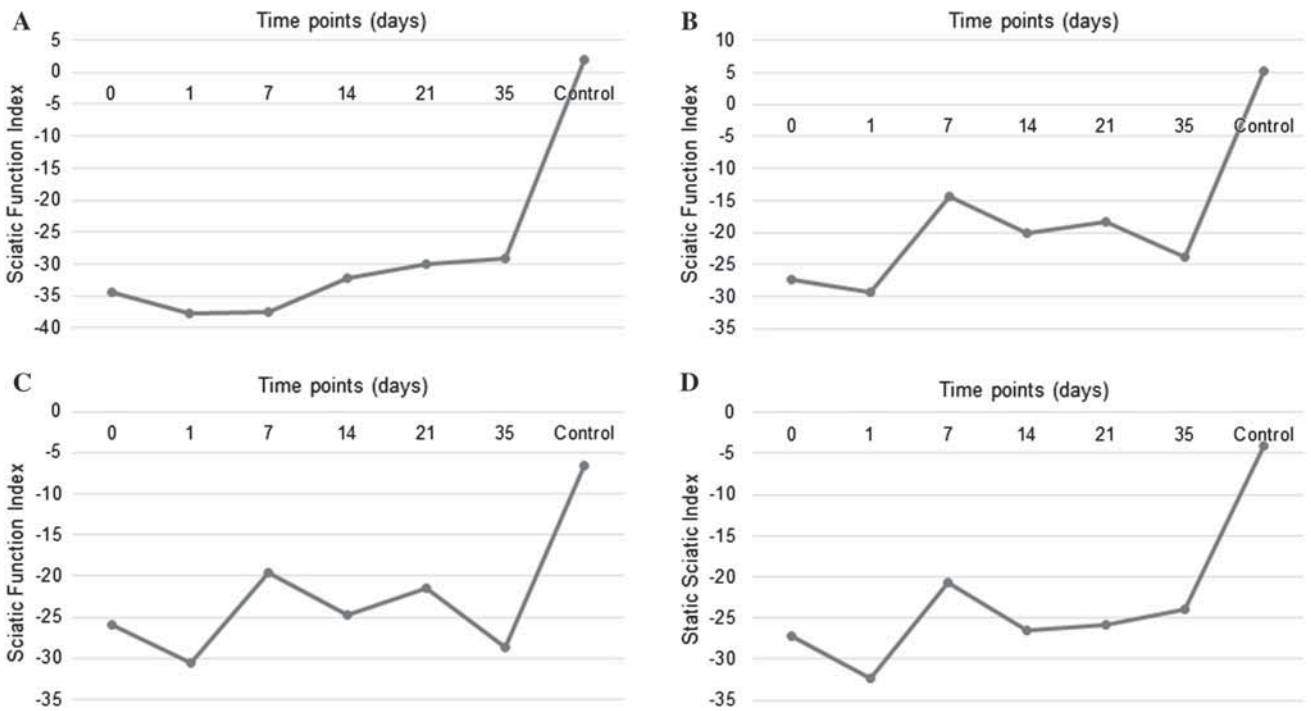

Figure 1. Sciatic function index (SFI) and Static sciatic index (SSI) alteration graphics calculated at 0 (3 h), 1, 7, 14, 21 and 35 days according to the (**A**) de Medinaceli *et al.* (1982), (**B**) Carlton and Goldberg (1986), (**C**) Bain, Mackinnon and Hunter (1989), and (**D**) Bervar (2000) formulas. Walking tracks of 7, 14, 21 and 35 days were recorded in 2-day intervals for all time points until the experimental endpoint. The average values of six individual walking tracks for each time point were used to calculate the SFI and SSI scores. The increase of these scores from negative to positive values during the time course indicate sciatic nerve recovery of newts after transection damage.

further proteomic analyses and to avoid individual differences. The control group was the left sciatic nerve, while both the distal and proximal nerve ending groups were the right sciatic nerve. The sciatic nerve tissues from the control and experimental groups were cut into small pieces with a surgical lancet, pulverized in liquid nitrogen, and homogenized in lysis buffer with ultrasonication. Afterward, samples were centrifuged for 45 min at 4 °C, 16,000*g*. The protein concentration of each sample was determined by the Bradford Protein Assay at 595 nm wavelength. Bovine serum albumin was used as a standard (Karahisar Turan *et al.* 2015; Peker *et al.* 2012).

2.7 *Two-dimensional gel electrophoresis (2D-PAGE)*

Experiments employing 2D-PAGE were performed with 7 cm linear immobilized pH gradient (IPG) strips (pH 3–10, Bio-Rad). Three technical replicates were prepared for each group, composed of six newt sciatic nerves. Forty-five µg proteins per gel were rehydrated actively at 50 V for 16 hours with rehydration buffer. Isoelectric focusing (IEF) and two-dimensional gel electrophoresis were performed following the protocols described at Karahisar Turan *et al.* (2015). Gels were stained with Oriole Fluorescent Gel Stain (Bio-Rad) for 90 min. Images were acquired with VersaDoc 1000 Imaging System (Bio-Rad) and were analyzed using PDQuest 8.0.1 Software (Bio-Rad Laboratories, USA). The expression level differences of protein spots between groups were analyzed with IBM SPSS Statistics Version 20 software. Descriptive statistics were performed to check for normal distributions using the Shapiro-Wilk test. Normally distributed continuous variables were compared with one-way ANOVA and post-hoc tests. $P<0.05$ was considered statistically significant.

2.8 *In-gel digestion and matrix assisted laser desorption ionization time-of- flight (MALDI-TOF) mass spectrometry*

Selected protein spots were excised from gels using the Proteome Works Spot Cutter (Bio-Rad). The excised gel pieces were transferred to a V-bottom 96-well plate. In-gel digestion was conducted according to Shevchenko *et al.* (1996) with some modifications, as explained in Karahisar Turan *et al.* (2015). Mass spectrometric analysis was performed in positive ion reflectron mode with a Waters Micromass MALDI-TOF. For external calibration, substance P, angiotensin, renin, ACTH, and glu-fib mixture were used.

Protein identifications were performed by Peptide Mass Fingerprint (PMF) analysis, using the MASCOT (*http://www.matrixscience.com*) server against UniProtKB (*http://www.uniprot.org*) database according to the raw spectra obtained from MassLynx 4.0 software. All searches were carried out for *Xenopus laevis*, the closest species to the *Triturus* genus in the database.

3. Results

3.1 *Walking track analysis*

The average SFI values of newts, which were separately calculated with four different formulas prior to sciatic nerve damage, ranged from −6.6 to 5.3. After transection, the SFI values decreased from healthy nerve values to −25.9 to −34.5 levels at the day 0 (3-hour) group. As regeneration proceeded, SFI values were ranged between −23.8−29.1 in the day 35 group, without statistically significant difference ($P>0.05$).

Figure 1 shows the alteration of SFI and SSI values for different time points which culminates at 35 days. Although the results do not exactly correlate with rat scores, the SFI graphs indicate that the values were gradually closer from negative to positive values. Therefore, this gradual increase reflects the recovery of damaged sciatic nerves in newts.

3.2 *Electrophysiological measurements*

Electrophysiological recordings were performed on both legs of each individual at six time points. After transecting the sciatic nerves at the 0 and 1 day groups, stimulation did not elicit the expected response. For other time points, averages from ten CMAP waves recorded from each individual were used to represent the amplitude and latency alteration in graphs.

The representative graphs of CMAP recordings of time points (7, 14, 21, and 35 days) and control values are shown in figure 2. The amplitude versus time point graph shows that amplitudes are gradually increased over time (figure 3). In a similar manner, the duration versus time point graph indicates that the duration is increased as the regeneration period progresses (figure 4). The difference of amplitude and duration values between time points was statistically significant ($p<0.05$). These findings correlated with the expected regeneration period of newts. As the neural damage recovered, amplitude and duration values were increased and approached control values. The same statistical analysis was performed for latency values; however, the difference was not significant between time points ($p>0.05$).

3.3 *Protein profiles*

Considering the protein profile maps, protein spots are distributed between 20–200 kDa, mostly between 40–80 kDa and pH 4–8 (figure 5). The horizontal chains in protein profiles indicate the possible appearance of isoforms or post-translational modifications that is known to have great importance in axonal regeneration. A total of 138 protein spots were matched between all groups by PDQuest analysis.

A comparison of the distal nerve ending groups at different time points indicates that 28 protein spots have statistically significant expression level differences between

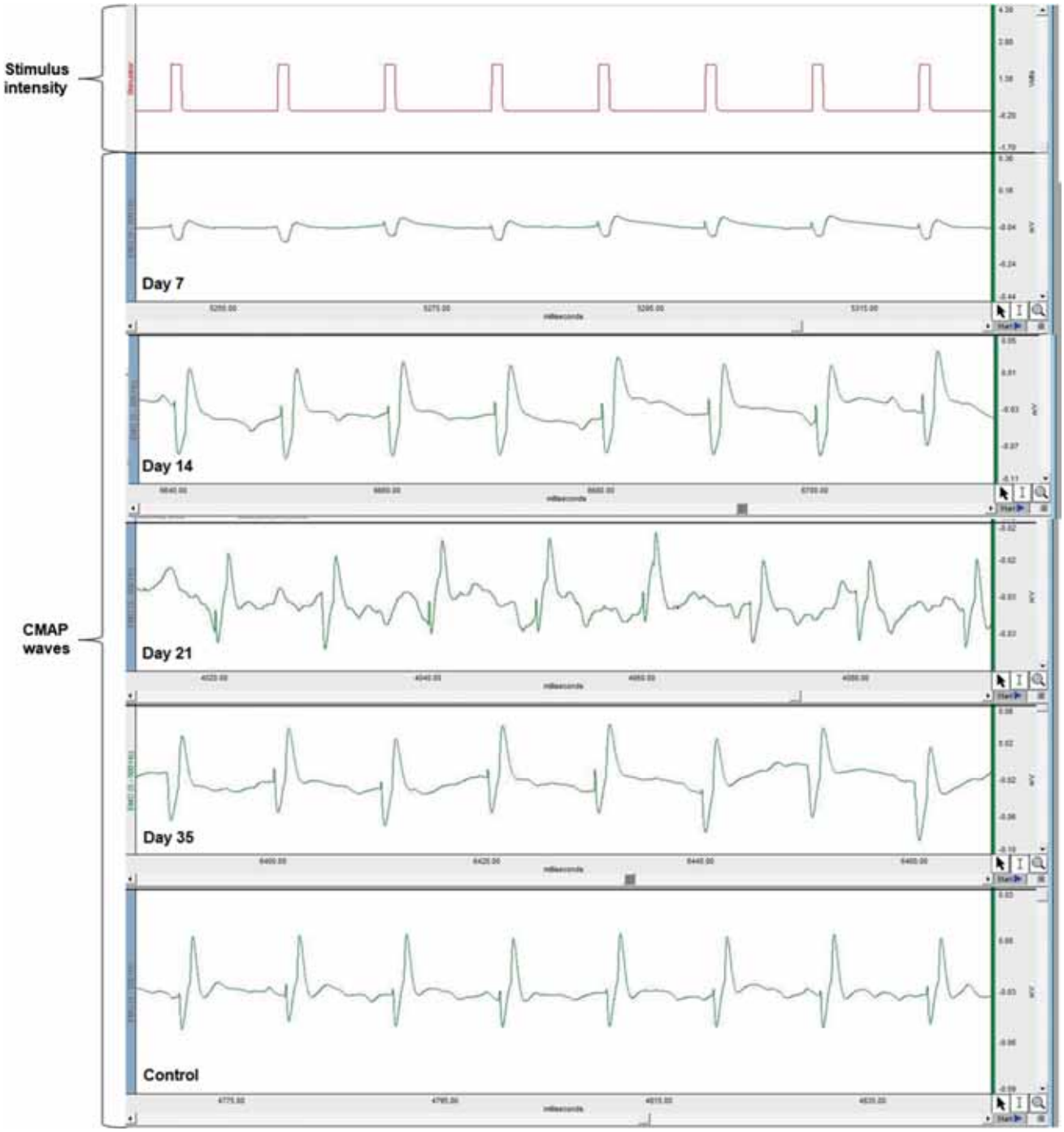

Figure 2. Representative graphs of CMAP recordings at four time points (7, 14, 21, and 35 days) where amplitude response could be elicited. No amplitude wave arose in the recordings of 0 and 1 day groups due to the transected sciatic nerves. The amplitude, duration, and latency values were calculated to monitor the recovery period after the sciatic nerve damage.

each other, and 38 protein spots between the proximal nerve ending groups ($p<0.05$).

3.4 *Protein identification by MALDI-TOF MS*

A total of 34 proteins were identified in this study (figure 6; table 1). To the best of our knowledge, the protein profile of the sciatic nerve tissue of *Triturus ivanbureschi* was examined for the first time in this study. For this reason, both the protein spots which have statistically different expression levels, and the remaining protein spots that can be excised from the gels were used in peptide mass fingerprint studies.

Differences in the expression level of protein spots for which protein identifications were executed, are shown in graphics using the density values in PDQuest (figure 7). For

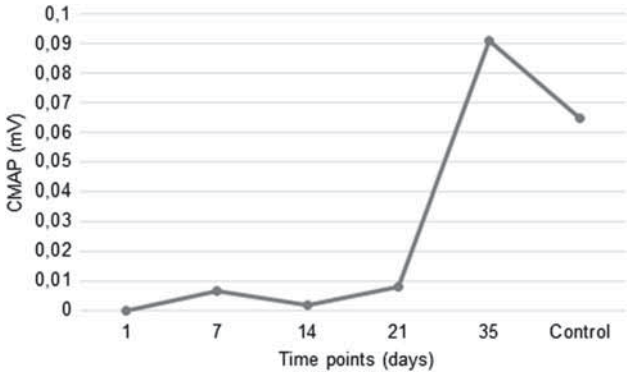

Figure 3. Amplitude (CMAP) variations at five time points (1, 7, 14, 21 and 35 days). The average values of damaged sciatic nerves are shown for five time points and the average values of non-operated sciatic nerves are used as control. Note the increasing amplitude values over time due to the recovery of sciatic nerves after transection. The difference of amplitude values between time points was statistically significant ($p<0.05$).

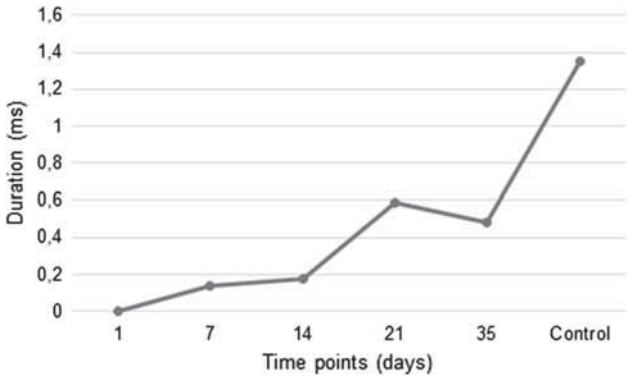

Figure 4. Variations in the duration period at five time points (1, 7, 14, 21 and 35 days). The average values of damaged sciatic nerves are shown for five time points; the average values of non-operated sciatic nerves are used for control. Increasing values of duration in time represent the success of sciatic nerve regeneration period after transection damage. The difference of duration values between time points was statistically significant ($p<0.05$).

each protein spot, the distal and proximal nerve ending values were evaluated at five time points. The distal and proximal endings of the sciatic nerves were integrated at 35 days, therefore the nerves of this group were analyzed together and the 35-day results were not provided in figure 7.

With respect to neural regeneration, the identified proteins were classified as: cytoskeletal, proteins with enzymatic-related activities, ubiquitination-associated, signal molecules and receptors, transport, cell adhesion and regulatory proteins (figure 8).

4. Discussion

The recovery period after peripheral nerve damage can be monitored by noninvasive methods, such as electrophysiological measurements and behavioral tests. In addition,

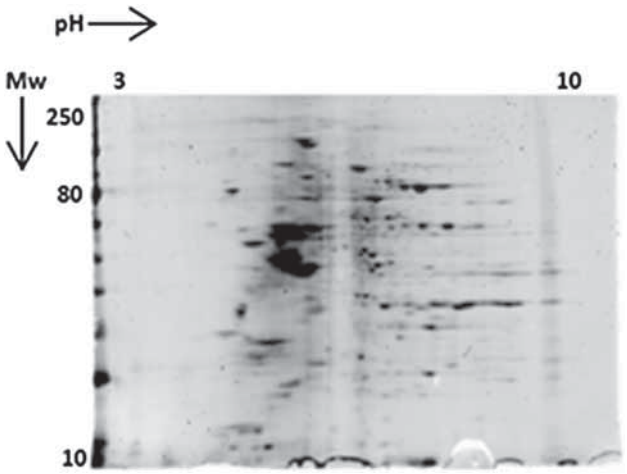

Figure 5. Representative protein profile map of *Triturus ivanbureschi* sciatic nerve tissue. This Oriole-stained gel is one of three replicates at day 1 in the distal nerve ending group. Total protein concentration loaded on this gel (7 cm linear immobilized pH gradient (IPG) strips, pH 3–10, Bio-Rad) was 45 µg. Note the protein spots are mostly distributed between 40–80 kDa and pH 4–8.

clarification of the underlying molecular mechanisms by transcriptomic and proteomic analysis may leads to successful neural regeneration treatments. To define the regeneration period after transection of *T. ivanbureschi* sciatic nerves, we performed a comprehensive study in which walking track analysis and electrophysiological recordings were used to monitor the healing period, and proteomic analysis were used for interpreting the regeneration mechanism.

Electrophysiological measurements, histomorphometry, and functional tests such as walking track analysis, are widely used in neural regeneration studies to obtain quantitative data (Sarikcioglu *et al.* 2009). There are many neural regeneration studies in the literature where walking track analysis is used to evaluate the sciatic nerve regeneration process in rats; however, for salamander models these studies are scarce. Kropf *et al.* (2010) used functional, electrophysiological, and radiographic measurements to identify the degree of recovery and time in axolotls after inflicting different type of sciatic nerve damage. Our study showed that the average SFI and SSI of healthy newts are close to the expected value, which corresponds to zero. However, the results of the day 35 group deviated significantly from the expected values. A rationale for this could be the walking pattern differences between newts and rats, whereby all four formulas in the literature for SFI and SSI are based on rats. We expected the SFI and SSI values of the transected sciatic nerves to be −100 but found the lowest average corresponded to – 34.5. If we consider this value as – 100, then the sciatic nerve recovery rate over a 35-day period corresponded to $\sim$30 %. The transected sciatic nerve stumps were physically combined by post-surgery day 35, when the study was terminated. We speculated that even

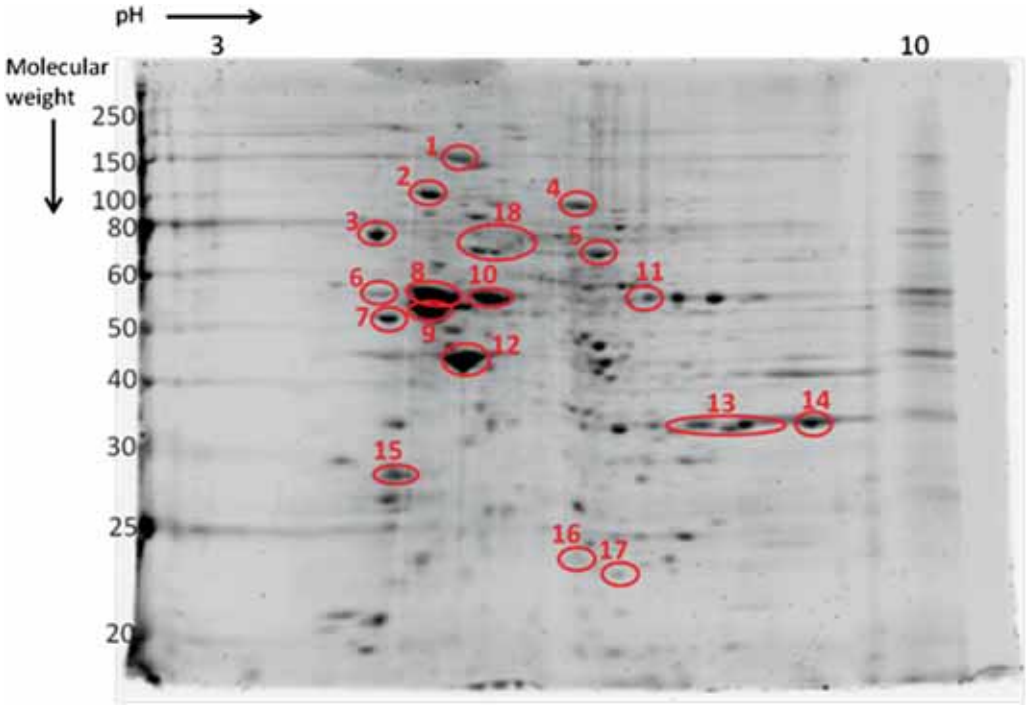

Figure 6. The locations of the protein spots where protein identifications were performed are marked on the gel. A total of 18 protein spots were excised from the gels and subsequently analyzed by mass spectrometry. The numbers in the gel correspond to the spot numbers listed in Table 1.

though anatomical continuity is restored sufficiently, more time is required for a complete functional recovery.

Electrophysiological measurements are generally used for the precise diagnosis of most neural system damage and disease; it is also an important tool to obtain quantitative data. Vleggeert-Lankamp (2007) published peripheral nerve regeneration studies between 1975 and 2004 and found that the latency and amplitude of CMAP waves can be readily measured. In this study, we measured both amplitude, duration and latency values, and found increased amplitude and duration values over time, but no significant change in latency values. The results of CMAP measurements indicate the repairing process after a serious neural damage in this species.

We identified 34 proteins with active roles in cellular regulation, developmental and metabolic processes, and biogenesis. According to the results of our study, while microenvironment regulatory proteins, transport proteins, growth factors, and guidance molecules of newly elongated neurites were highly expressed from distal nerve ending groups, morphoregulatory proteins, proteins associated with neurite elongation, and especially cytoskeletal proteins were highly expressed in the proximal nerve ending groups. Our findings on the expression level differences of distal and proximal nerve endings reaffirms the diverse responses of distal and proximal sprouts after transection injuries.

Many researchers focus on the unknown mechanisms of neural regeneration. The field has determined that successful regeneration is dependent on several types of proteins, including neurotrophins, neuropoietic cytokines, growth-associated proteins, cytoskeletal proteins, neuropeptides, cell adhesion molecules, etc. (Fu and Gordon 1997). Furthermore, the functional transcriptional pathways in peripheral nerve regeneration include cAMP/PKA/CREB, JNK/c-Jun, ATF3, JAK/STAT3, Ac-p53, BMPs/Smad1 (Tedeschi 2012).

According to the molecular functions of gene ontology database, 21 of the identified proteins have binding activity, ten have catalytic activity, five have structural molecule activity, two have molecular transducer activity and one has enzyme regulator activity. These proteins also function in cellular regulation, developmental and metabolic processes, and biogenesis. In our study, the expression levels of cytoskeletal proteins like tubulin chains, actin, peripherin, vimentin and nexin are higher both in distal and proximal nerve endings than control groups. Axotomy causes an increase in the expression levels of cytoskeletal proteins, such as actin and tubulin forms, to reorganize the growing axons. For a successful regeneration, axotomized neurons should transform from transmitting mode to growing mode and support the axonal regeneration. Casein kinase II expression levels are activated by nerve growth factors, support axonal elongation and function in the regulation of cytoskeletal modifications and are also increased in damaged axons compared to controls in this study. These findings are compatible with the literature, where it is reported that increased expression and rearrangement of cytoskeletal-related proteins accelerates the neurite elongation process (Fu and Gordon 1997; Zochodne 2008).

Table 1. List of identified proteins by MALDI-TOF MS

Protein spot number	SwissProt Accession number	Identified protein	Score	Theorethical pI/MW (kDa)	Experimental pI/MW (kDa)	Protein sequence coverage (%)	Matched/ Unmatched Peptide	Functional Classification
8	TBA_XENLA	Tubulin alpha chain	150	4.96/50.5	5.0/57.8	33	10/4	Cytoskeletal proteins
9	TBB2_XENLA	Tubulin beta-2 chain	103	4.81/50.1	5.0/53.8	27	8/9	
12	ACTB_XENLA	Actin, cytoplasmic 1	52	5.30/42.1	5.3/42.7	17	5/19	
10	PERI_XENLA	Peripherin	43	5.23/52.1	5.5/57.4	15	9/46	
5	FASC_XENLA	Fascin	21	7.05/53.6	6.4/73.9	7	2/11	
10	VIM1_XENLA	Vimentin-1/2	15	5.16/52.9	5.5/57.4	5	2/15	
11	5NTC_XENLA	Cytosolic purine 5'-nucleotidase	40	5.45/66.7	6.9/58.8	13	5/14	Enzyme activity
18	RAGP1_XENLA	Ran GTPase-activating protein 1	33	4.53/63.5	5.4/73.8	10	5/19	
14	CSK21_XENLA	Casein kinase II subunit alpha	32	7.29/45.3	8.4/36	11	3/9	
18	EPHB3_XENLA	Ephrin type-B receptor 3	27	5.71/109.7	5.4/73.8	6	5/18	
13	RD10A_XENLA	Retinol dehydrogenase 10-A	19	7.89/39.2	7.4/35.9	7	2/10	
16	FXL15_XENLA	F-box/LRR-repeat protein 15	35	6.69/33.8	7.0/27.0	12	2/4	Ubiquitination associated proteins
3	TRF6B_XENLA	TNF receptor-associated factor 6-B	23	5.84/65.0	4.5/80	4	2/4	
13	TM129_XENLA	E3 ubiquitin- protein ligase TM129	17	7.57/41.8	7.4/35.9	3	2/9	
11	ESR1_XENLA	Estrogen receptor	24	7.59/66.8	6.9/58.8	5	3/16	Signal molecules and receptors
6	FGFR4_XENLA	Fibroblast growth factor receptor 4	22	5.36/94.4	5.4/73.8	5	4/19	
15	PENKA_XENLA	Proenkephalin-A-A	20	5.16/30.4	4.7/31.1	6	3/10	
10	ACHAA_XENLA	Acetylcholine receptor subunit alpha-1-A	20	6.17/52.8	5.5/57.4	8	2/15	
17	NRN1B_XENLA	Neuritin- B	16	6.06/16.2	6.5/24.5	15	1/10	
4	XPO7B_XENLA	Exportin-7-B	32	5.84/124.6	6.2/133.3	4	3/5	Transport proteins
17	RAB19_XENLA	Ras-related protein Rab- 19	26	6.38/24.3	6.5/24.5	15	2/9	
1	CAPS1_XENLA	Calcium-dependent secretion activator 1	22	5.50/149.8	5.20/150	3	4/14	
10	SNX33_XENLA	Sorting nexin-33	16	5.99/63.5	5.5/57.4	5	1/16	
2	CTNA2_XENLA	Catenin alpha-2	30	5.52/107.8	5/111.2	5	3/13	Cell-adhesion molecule
11	GNL3_XENLA	Nucleostemin like protein	27	8.37/61.6	6.9/58.8	6	3/16	Regulatory proteins
11	PALM3_XENLA	Paralemmin-3	24	4.66/66.5	6.9/58.8	5	3/16	
6	ZBT18_XENLA	Zinc finger and BTB domain- containing protein 18	21	5.66/59.6	4.5/57.3	6	2/5	
18	AB1IP_XENLA	Amyloid beta A4 precursor protein binding family B member 1-interacting protein	21	6.02/73.1	5.4/73.8	7	3/ 20	
6	ECSIT_XENLA	Evolutionary conserved signaling intermediate in Toll pathway, mitochondrial	20	5.55/48.0	4.5/57.3	9	2/5	
7	TGFI1_XENLA	Transforming growth factor beta- 1- induced transcript 1 protein	19	5.61/57.6	4.6/51.5	5	2/13	
13	HM20A_XENLA	High mobility group protein 20A	18	6.86/39.7	7.4/35.9	4	2/9	
4	CHRD_XENLA	Chordin	18	6.17/107.5	6.2/133.3	4	3/5	
11	RCOR2_XENLA	REST corepressor 2	16	7.16/56.3	6.9/58.8	7	3/16	
16	F206A_XENLA	Protein Simiate	15	7.55/21.2	7.0/27.0	8	1/5	

Experimental pI/MW (kDa) values are obtained from the PDQuest 8.0.1 software. Raw spectra of peptide masses are obtained from MassLynx 4.0 software. Peptide Mass Fingerprint (PMF) analysis was performed using the MASCOT server against UniProtKB (*http://www.uniprot.org*) database. All searches were carried out for *Xenopus laevis*. Protein spot numbers are available in figure 6

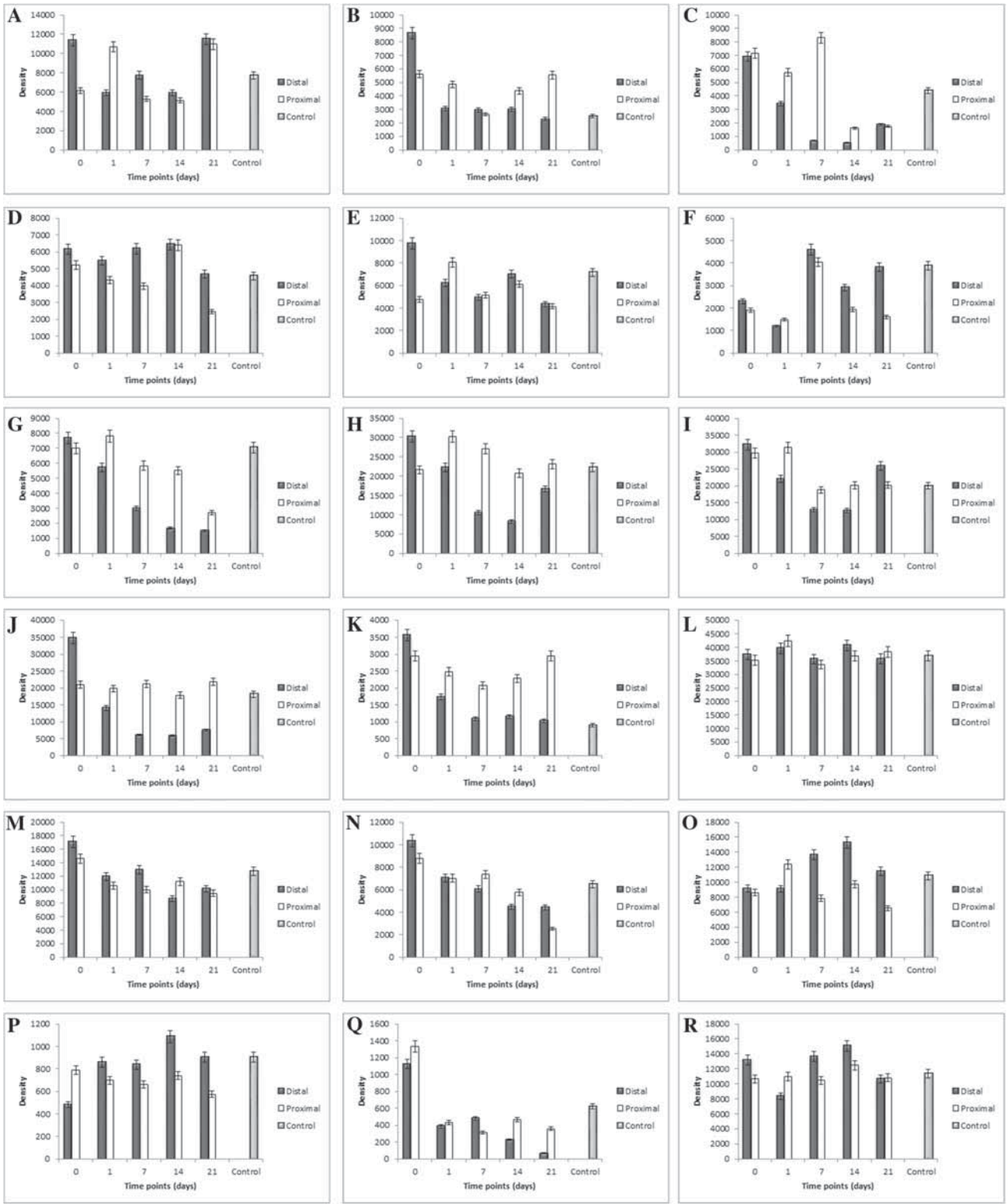

Figure 7. Altered expression level in protein spots at five time points (0, 1, 7, 14 and 21 days) where protein identifications were performed. White bars represent the proximal nerve ending groups; dark gray bars, distal nerve ending groups; light gray bars, results control group. Density values of selected spots were taken from the PDQuest 8.0.1 software. More than one protein was identified from some spots; therefore, the expression levels were arranged by spot numbers. The alphabetical order of graphs (**A–R**) is consistent with the protein spot numbers (1–18), which was indicated in figure 6. There was only one bar for control groups per graph, because the average values of control groups at different time points were used.

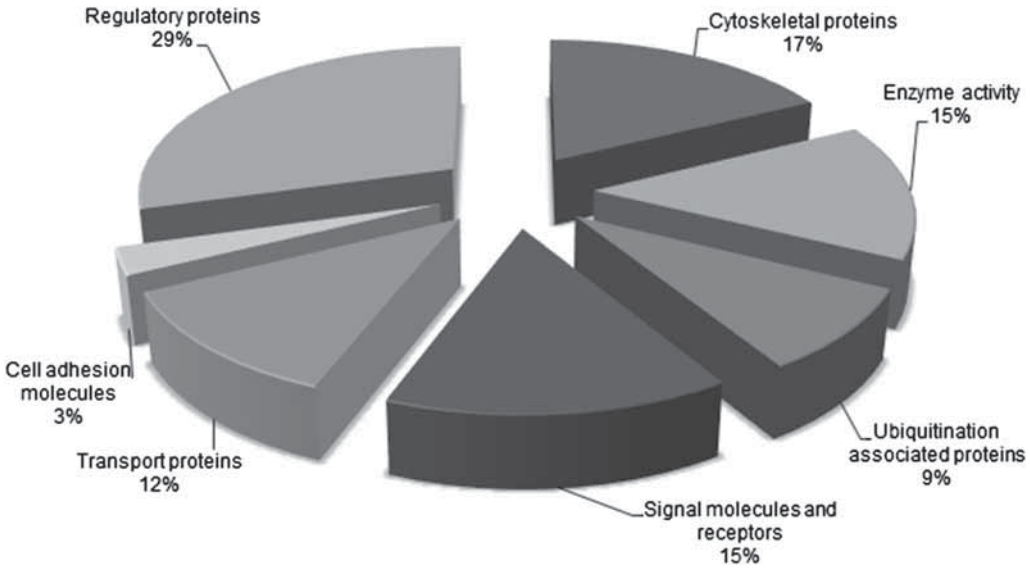

Figure 8. Functional classification of the 34 proteins identified in this study. Numbers in the pie charts represent the percentages of total proteins.

Differences in protein expression levels in between distal and proximal nerve endings are represented: microenvironmental regulatory and guidance molecules for recently emerging neurites are secreted from distal nerve endings while molecules concerned with neurite elongation (like cytoskeletal proteins) are highly expressed in proximal nerve endings. The expression levels of tubulin isoforms alpha and beta-2 chains, actin, peripherin, vimentin, nexin and fascin are higher in proximal nerve endings than distal endings at one or more time points. TNF receptor-associated factor 6-B is a ubiquitin kinase that is efficient in neural development and is also highly expressed in proximal nerve endings in comparison with distal ones.

The expression level of fibroblast growth factor receptor 4 are higher in proximal nerve endings than distal endings, except at the day 1 group. The members of this protein family are functional in tissue repair and trigger the injury-induced response. According to the literature, the expression levels of these proteins are increased after damage to both distal and proximal nerve endings (Eswarakumar *et al.* 2005; Grothe and Nikkhah 2001; Zhang *et al.* 2002). The alteration of expression levels of this protein is also assumed as an indicator of the axonal regeneration in this study.

Transforming growth factor beta-1 induced transcript 1 appeared in many tissues as a regulator of cell growth and differentiation. In peripheral nerve tissues, it is responsible for inducing the regenerative response followed by Wallerian degeneration, and regulates the Wnt and steroid pathways (Einheber *et al.* 1995). In this study, the expression levels are higher in proximal nerve endings than distal ones at all-time points, except the day 0 group.

Cytosolic purine 5'-nucleotidase has trophic effects on neurite elongation (Zimmermann 1996). The expression levels of this molecule are higher in proximal, rather than distal nerve ending groups, except the day 0 group. Paralemmin, a morphoregulator protein efficient in neurite elongation, also has the same expression pattern. Another identified protein that showed a similar expression pattern is estrogen receptor, which is expressed from Schwann cells and increased Schwann cell proliferation (Bhattacherjee *et al.* 2014; Melcangi *et al.* 2005). Simultaneously, the estrogen receptor expression level gradually decreased as regeneration progressed in distal nerve endings.

Transport proteins, growth factors, signal molecules, and regulatory molecules were increased in distal nerve endings compared to proximal nerve endings. These include F-box/LRR-repeat protein 15, which is functional in BMP pathway; the simiate protein, which regulates transcriptional activity and actin polymerization; exportin, which transports proteins and RNA molecules between the cytoplasm and nucleus in eukaryotic cells; chordin, which is an important molecule for the regulation of extracellular signals; Ras-related protein Rab-19; and neuritin-B. Rab proteins have GTP-binding activities and they regulate vesicle movements (Pereira-Leal and Seabra 2001). In addition, it is known that neuritin expression is increased after damage and neuritin can be transported bidirectionally through the axons (Karamoysoyli *et al.* 2008; Shimada *et al.* 2013). Calcium-dependent secretion activator 1 plays a role in the exocytosis of neurotransmitters and neuropeptide vesicles (Loyet *et al.* 1998), and its expression levels are higher in distal rather than proximal nerve endings at more than one time point in our study.

Zinc finger and BTB domain-containing protein 18 functions as a transcriptional inhibitor and shows higher expression levels in distal rather than proximal nerve endings in all groups except the day 1 group. Evolutionary conserved signaling intermediate in Toll pathway and

proenkephalin are two other identified proteins that show the same expression profiles. Evolutionary conserved signaling intermediate in Toll pathway protein is functional in both the Toll-like and BMP pathways (Vogel *et al.* 2007) and the expression of proenkephalin is regulated by growth factors and neurotrophic factors (Tan *et al.* 1994).

The deficiency of successful regeneration in mammal associates with the absence of the blastema formation, which is the source of cells for regeneration, and fast fibroproliferative response after injury (Kumar *et al.* 2010). The success of peripheral nerve regeneration attributes to the removal of axon and myelin debris and the growth environment in the distal nerve stump. Regenerated axons grow through the denervated targets inside of the endoneural tubes formed by steady axons and myelin sheats. In crush injuries, the continuity of endoneural tubes is protected. Therefore, crush injuries can result with successful regeneration and functional recovery in mammals. However, in transection damages the neural sheat breaks off and a surgical repair is needed to obtain a successful regeneration in mammals. The regenerated axons should pass the gap between the distal and proximal nerve endings in the transected nerves. While proliferated Schwann cells and fibroblasts migrate both from distal and proximal nerve stumps and form a cell-matrix layer in this gap, the number of regenerated axons that can pass this gap successfully still stays under the optimum number. Besides, this gap reduces the possibility of regenerated axons growing to their original endoneural tubes. Lots of branches are formed from the regenerated axonal roots and they enter into empty endoneural tubes randomly. As a result of this, regenerated axons cannot reinnervate their original targets and this misorientation is known as the major problem of inadequate functional regeneration in mammals (Fu and Gordon 1997). Besides, amphibian regeneration is considered to be mediated by extensive cellular transdifferentiation. The differentiated cells in the amputation site firstly de-differentiate and then re-differentiate again to form the lost part of the body. This transdifferentiation mechanism can't occur in many mammalian tissues (Alvarado and Tsonis 2006).

In conclusion, the present study has revealed that newt is a good model organism for investigating the sciatic nerve regeneration period, especially in transection damage models. Taken together, these results from behavioral, electrophysiological and proteomic studies demonstrate the repairing process of sciatic nerves after transection damage. To our knowledge, the proteome of *T. ivanbureschi* sciatic nerve was investigated for the first time. Although the distal and proximal nerve endings are connected in 35 day periods after transection, the results of behavioral analysis and electrophysiological recordings showed that more time is needed for complete, functional regeneration. The expression levels of certain proteins differ between distal and proximal nerve endings at different time points. While transport proteins, growth factors, signaling, and regulatory molecules were highly expressed in distal nerve stumps, proteins related with the neurite elongation process, especially cytoskeletal proteins, were highly expressed in proximal nerve stumps. In conclusion, identified proteins in this study are functional in PKB/AKT, CaMKK/AMPK and STAT-5 signaling pathways. Our work should serve as a starting point for future nervous system regeneration studies on amphibians, which can help illuminate the complex molecular mechanism of the neural regeneration process.

Acknowledgements

This work was supported by The Scientific and Technological Research Council of Turkey (TÜBİTAK) [Grant Number 113Z124] and is also part of a doctorate thesis (Seçil Karahisar Turan, Hacettepe University, Institute of Science). We are grateful to Dr. Ali Demirsoy for his great, *ad hoc* counseling. We also thank Beycan Ayhan, Hatice Yıldızhan, Naşit İğci, N. Pınar Barkan and Selen Peker for technical expertise. This study was funded by The Scientific and Technological Research Council of Turkey (TÜBİTAK) [Grant Number 113Z124].

Compliance with ethical standards

Ethical approval All *Triturus ivanbureschi* specimens were collected from their natural habitats with the permission of the Republic of Turkey, Ministry of Forestry and Water Affairs, General Directorate of Nature Conservation and National Parks (protocol B.23.0.DMP.0.15.01-510.02-9165). All experimental procedure was approved by Hacettepe University Animal Research Ethics Committee (protocol B.30.2.HAC.0.05.06.00/17).

References

Alvarado AS and Tsonis PA 2006 Bridging the regeneration gap: genetic insights from diverse animal models. *Nat. Rev. Genet.* **7** 873–884

Bain J, Mackinnon S and Hunter D 1989 Functional evaluation of complete sciatic, peroneal, and posterior tibial nerve lesions in the rat. *Plast. Reconstr. Surg.* **83** 129–136

Bervar M 2000 Video analysis of standing–an alternative footprint analysis to assess functional loss following injury to the rat sciatic nerve. *J. Neurosci. Methods* **102** 109–116

Bhattacherjee A, Liao Z and Smith PG 2014 Trophic factor and hormonal regulation of neurite outgrowth in sensory neuron-like 50B11 cells. *Neurosci. Lett.* **558** 120–125

Carlson B 2007 *Principles of regenerative biology* (Academic Press, USA)

Carlton J and Goldberg N 1986 Quantitating integrated muscle function following reinnervation. *Surg. Forum* **3** 611–612

de Medinaceli L, Freed WJ, Wyatt RJ 1982 An index of the functional condition of rat sciatic nerve based on measurements made from walking tracks. *Exp. Neurol.* **77** 634–643

Einheber S, Hannocks M-J, Metz CN, Rifkin DB and Salzer JL 1995 Transforming growth factor-beta 1 regulates axon/Schwann cell interactions. *J. Cell Biol.* **129** 443–458

Eswarakumar V, Lax I and Schlessinger J 2005 Cellular signaling by fibroblast growth factor receptors. *Cytokine Growth Factor Rev.* **16** 139–149

Fu SY and Gordon T 1997 The cellular and molecular basis of peripheral nerve regeneration. *Mol. Neurobiol.* **14** 67–116

Goto A, Wang YL, Kabuta T, Setsuie R, Osaka H, Sawa A, Ishiura S and Wada K 2009 Proteomic and histochemical analysis of proteins involved in the dying-back-type of axonal degeneration in the gracile axonal dystrophy (gad) mouse. *Neurochem. Int.* **54** 330–338

Grothe C and Nikkhah G 2001 The role of basic fibroblast growth factor in peripheral nerve regeneration. *Anat. Embryol.* **204** 171–177

Karahisar Turan S, Ali Onur M, Demirsoy A and Ozel Demiralp, D 2015 Proteomic comparison of damaged sciatic nerves of a newt, *Triturus karelinii* (Amphibia: Urodela) during the first 24th hour of regeneration period. *Curr. Proteomics* **12** 273–279

Karamoysoyli E, Burnand RC, Tomlinson DR and Gardiner NJ 2008 Neuritin mediates nerve growth factor–induced axonal regeneration and is deficient in experimental diabetic neuropathy. *Diabetes* **57** 181–189

Kiffmeyer WR, Tomusk EV and Mescher AL 1991 Axonal transport and release of transferrin in nerves of regenerating amphibian limbs. *Dev. Biol.* **147** 392–402

Kropf N, Krishnan K, Chao M, Schweitzer M, Rosenberg Z and Russell SM 2010 Sciatic nerve injury model in the axolotl: functional, electrophysiological, and radiographic outcomes: Laboratory investigation. *J. Neurosurg.* **112** 880–889

Kumar V, Abbas AK, Fausto N and Aster J 2010 *Tissue renewal, regeneration and repair pathologic basis of disease* 8th edn (Elsevier, Philadelphia) pp79–110

Loyet KM, Kowalchyk JA, Chaudhary A, Chen J, Prestwich GD and Martin TF 1998 Specific binding of phosphatidylinositol 4, 5-bisphosphate to calcium-dependent activator protein for secretion (CAPS), a potential phosphoinositide effector protein for regulated exocytosis. *J. Biol. Chem.* **273** 8337–8343

Lu A, Wiśniewski JR, Mann M 2009 Comparative proteomic profiling of membrane proteins in rat cerebellum, spinal cord, and sciatic nerve. *J. Proteome Res.* **8** 2418–2425

Melcangi RC *et al.* 2005 Peripheral nerves: a target for the action of neuroactive steroids. *Brain Res. Rev.* **48** 328–338

Michaelevski I, Medzihradszky KF, Lynn A, Burlingame AL and Fainzilber M 2010 Axonal transport proteomics reveals mobilization of translation machinery to the lesion site in injured sciatic nerve. *Mol. Cell Proteomics* **9** 976–987

Peker S, Akar N, Demiralp DO 2012 Proteomic identification of erythrocyte membrane protein deficiency in hereditary spherocytosis. *Mol. Biol. Rep.* **39** 3161–3167

Pereira-Leal JB and Seabra MC 2001 Evolution of the Rab family of small GTP-binding proteins. *J. Mol. Biol.* **313** 889–901

Rodríguez FJ, Valero-Cabré A and Navarro X 2004 Regeneration and functional recovery following peripheral nerve injury. *Drug Discov. Today Dis. Models* **1** 177–185

Sarikcioglu L, Demirel B and Utuk A 2009 Walking track analysis: an assessment method for functional recovery after sciatic nerve injury in the rat. *Folia Morphol. (Warsz)* **68** 1–7

Shevchenko A, Wilm M, Vorm O, Mann M 1996 Mass spectrometric sequencing of proteins from silver-stained polyacrylamide gels. *Anal. Chem.* **68** 850–858

Shimada T, Sugiura H and Yamagata K 2013 Neuritin: A therapeutic candidate for promoting axonal regeneration. *World J. Neurol.* **3** 138–143

Tan Y, Low KG, Boccia C, Grossman J and Comb MJ 1994 Fibroblast growth factor and cyclic AMP (cAMP) synergistically activate gene expression at a cAMP response element. *Mol. Cell Biol.* **14** 7546–7556

Tedeschi A 2012 Tuning the orchestra: transcriptional pathways controlling axon regeneration. *Front Mol. Neurosci.* **4** 60

Tsonis PA 2002 Regenerative biology: the emerging field of tissue repair and restoration. *Differentiation* **70** 397–409

Vleggeert-Lankamp CL 2007 The role of evaluation methods in the assessment of peripheral nerve regeneration through synthetic conduits: a systematic review. *J. Neurosurg.* **107** 1168–1189

Vogel RO, Janssen RJ, van den Brand MA, Dieteren CE, Verkaart S, Koopman WJ, Willems PH, Pluk W, van den Heuvel LP, Smeitink JA and Nijtmans LG 2007 Cytosolic signaling protein Ecsit also localizes to mitochondria where it interacts with chaperone NDUFAF1 and functions in complex I assembly. *Genes Dev.* **21** 615–624

Wielstra B and Arntzen J 2016 Description of a new species of crested newt, previously subsumed in Triturus ivanbureschi (Amphibia: Caudata: Salamandridae). *Zootaxa* **4109** 73–80

Zhang F, Clarke J, Santos-Ruiz L and Ferretti P 2002 Differential regulation of fibroblast growth factor receptors in the regenerating amphibian spinal cord in vivo. *Neuroscience* **114** 837–848

Zimmermann H 1996 Biochemistry, localization and functional roles of ecto-nucleotidases in the nervous system. *Prog. Neurobiol.* **49** 589–618

Zochodne DW 2008 *Neurobiology of peripheral nerve regeneration* (Cambridge University Press, Cambridge)

Corresponding editor: Aurnab Ghose